

LETTER TO THE EDITOR

Use of minigene assays as a useful tool to confirm the pathogenic role of intronic variations of the *ANK1* gene: Report of two cases of hereditary spherocytosis

ANK1 is one of the most frequently mutated genes in hereditary spherocytosis (HS) in European countries and encodes the protein Ankyrin-1 which is a major membrane erythrocyte protein linking horizontal protein network to the vertical one. Inheritance can be either autosomal dominant or recessive depending on the type of variations.^{1,2} According to the American College of Medical Genetics and Genomics (ACMG) classification,³ loss of function variations (nonsense, frameshift, canonical splicing regions) of the *ANK1* gene is dominant and can be undoubtedly classified at least as probably pathogenic (class 4) in a context of HS. On the contrary, variations affecting deeper regions of introns cannot be classified higher than class 3 (variation of uncertain significance [VUS]) without functional characterization. We recently encountered that situation in two typical cases of HS (a 61-year-old man; patient 1 and a 15-year-old boy, patient

2). We performed NGS analysis targeting known genes implicated in red blood cell membrane diseases for these two patients (Supplementary data: NGS panel genes list). Molecular analysis revealed the presence of an *ANK1* intronic variation at heterozygous state: NM_020476 (*ANK1*): c.1405-9G>A (intron 13) in patient 1 and c.5097-33G>A (intron 38) in patient 2.

Both variations were absent in the gnomAD v3.1.2 database and all used splicing prediction software (Splice Site Finder-like, MaxEntScan, NNSPLICE, GeneSplicer) concluded to altered splicing (Figure 1). The intron 13 variation led to the decrease in the canonical acceptor site strength and to the creation of a new strong cryptic acceptor site, whereas the intron 38 variation led to the creation of a cryptic acceptor site with higher scores than the canonical one. Moreover, these two intronic *ANK1* variations had already

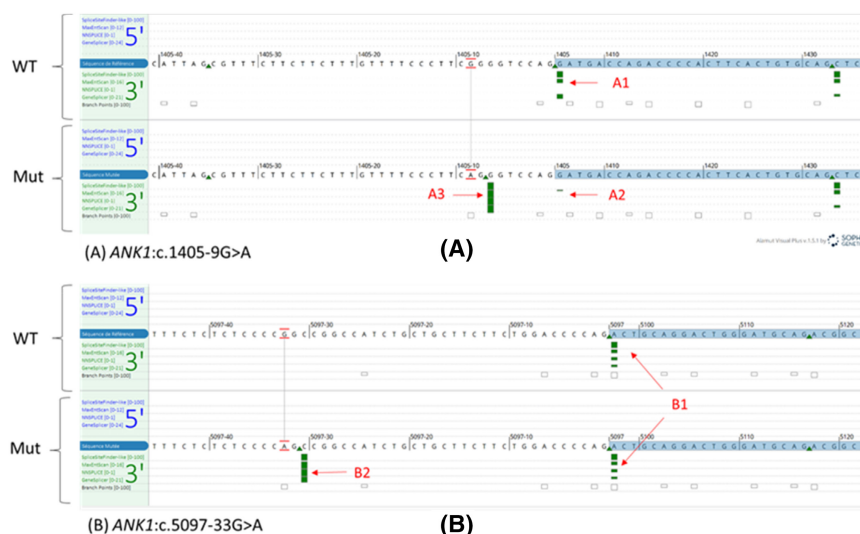


FIGURE 1 Screenshots from Alamut® interface representing splicing predictions of four different dedicated software for the two *ANK1* intronic variations. (A) *ANK1*:c.1405-9G>A and (B) *ANK1*:c.5097-33G>A. Each screenshot is divided into two parts: the upper part represents the splicing predictions of the wild-type (WT) sequence and the lower part those of the mutated (Mut) sequence. Each line corresponds to one particular software (namely Splice Site Finder-like, MaxEntScan, NNSPLICE and GeneSplicer), either for splicing donor sites (5' blue lines) or for splicing acceptor sites (3' green lines). The presence of a green rectangle indicates that the software predicts 3' splicing on that position. (A) The canonical acceptor site (A1) is abolished by the *ANK1*:c.1405-9G>A mutation (A2) and replaced by an alternative acceptor site 7 bp before (A3). (B) *ANK1*:c.5097-33G>A mutation does not modify the canonical acceptor site (B1) but creates an alternative site 31 bp before (B2). This alternative site seems to be stronger than the canonical one since the green rectangle scores are higher for all four software.

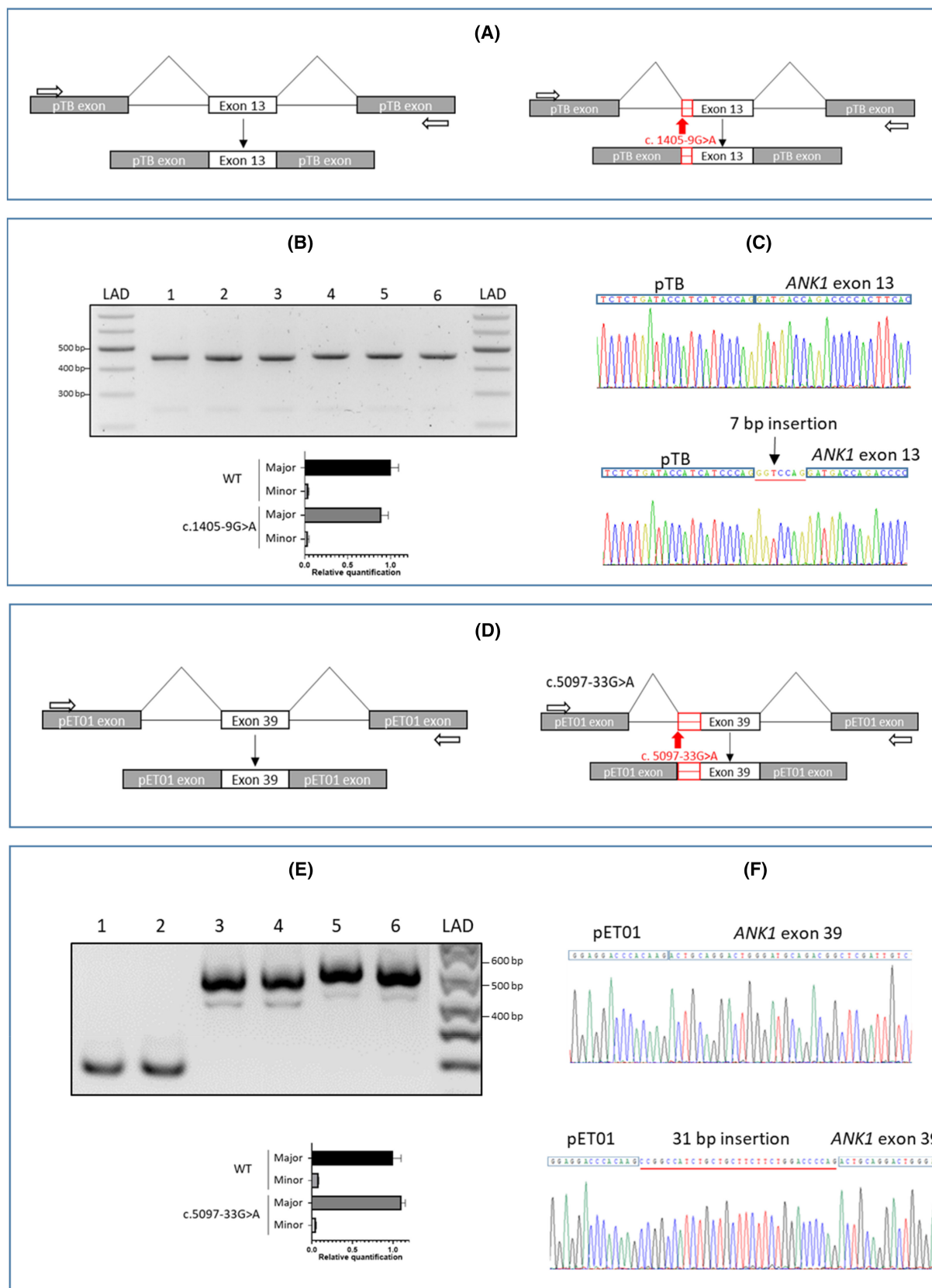


FIGURE 2 Representation of the hybrid minigene splicing assays for the *ANK1*:c.1405-9G>A and c.5097-33G>A variation. (A) Schematic representation of the minigene including *ANK1* exon 13 (white boxes) and intronic regions (black lines) for the wild-type and the mutated constructs. (B) RT-PCR results obtained after transfection of HeLa cells with wild-type (lanes 1 to 3) and mutated (lanes 4 to 6) construct for *ANK1*:c.1405-9G>A variation and relative quantification of the intensity of each band. (C) Sanger sequencing results of the major products obtained after transfection with wild-type and mutated construct. (D) Schematic representation of the minigene including *ANK1* exon 39 (white boxes) and intronic regions (black lines) for the wild-type and the mutated constructs. (E) RT-PCR results obtained after transfection of HeLa cells with empty pET01 vector (lanes 1 and 2), wild-type (lanes 3 and 4) and mutated (lanes 5 and 6) construct for *ANK1*:c.5097-33G>A variation and relative quantification of the intensity of each RT-PCR products obtained after transfection with wild-type and mutated construct. (F) Sanger sequencing results of the major products obtained after transfection with wild-type and mutated construct.

been referenced in a 2020 publication by Tole et al.⁴ who established a list of potentially implicated variations in a cohort of paediatric HS cases. Interestingly, thanks to the corresponding author, we learned that all the described HS patients harbouring the -33 variation were family related. Their common ancestor was a farmer who lived in Toronto region at the end of the 19th century, which strongly suggested a founder effect. The -9 variation was associated with a new HS description 1 year later in a Chinese family.⁵

Taken together, these arguments were strongly in favour of these two variations of causality in the diagnosis of HS. Unfortunately, no functional studies were performed in these two publications. We performed a minigenes analysis on both variations. Those results allowed us to reclassify it as pathogenic variations according to ACMG classification. It is to note that these two minigenes were performed in two distinct laboratories. The precise and complete description of each protocol is available in supplementary data but the principle remains the same. Briefly, total RNA was purified from cultured cells transfected with empty plasmid, minigene containing partial wild-type (WT) or mutated *ANK1* intron, prior natural *n*+1 exon and partial *n*+1 intron. RT-PCR products using primers located in the plasmid exons before and after the *ANK1* exon of interest were obtained (Figure 2A,D), analysed on agarose gel (Figure 2B,E) and sequenced using Sanger analysis (Figure 2C-F).

For the *ANK1*:c.1405-9G>A mutation (intron 13), both the normal and mutated minigene gives rise to a major RT-PCR product of about 450 bp which may correspond to the normal splicing of exon 14 (expected size = 445 bp) (Figure 2B). Interestingly, a very minor product of about 250 bp was also observed which may correspond to exon 14 skipping (expected size = 247 bp). Sanger sequencing confirmed these hypotheses but, for the 450-bp product of the mutated minigene, exon 14 was preceded by the last seven bases of intron 13 (Figure 2C). The *ANK1*:c.1405-9G>A mutation has thus a complete modifying effect on splicing with the exonisation of the 7 last bases of intron 13 that gives rise to a frameshift leading to a premature stop-codon a few bases later.

For the *ANK1*:c.5097-33G>A mutation (intron 38), the wild-type minigene gives a major RT-PCR product of 537 bp while the corresponding one for the mutated minigene was 31 bp longer (568 bp) (Figure 2E). A minor PCR product of about 411 bp for WT and 442 bp for mutated construct was also observed which may correspond to the creation of an artefactual donor site in the exon 39 sequence. It was thus confirmed that the *ANK1*:c.5097-33G>A mutation creates a new splicing site triggering

frameshift due to 31 bp insertion leading to a premature non-sense codon UGA in position c.5217 (p.1739) in exon 39 (Figure 2F).

No normal transcript was produced after the transfection of the mutated minigene.

In conclusion, our study proves again the high usefulness of minigenes studies in functional testing of intronic VUS in the field of hereditary hemolytic anaemia.⁶ It also emphasizes the importance of searching for deep intronic variations out of usual flanking intronic regions in next generation-sequencing analysis pipelines.

AUTHOR CONTRIBUTIONS

Ariane Lunati-Rozie wrote the paper, Alexandre Janin and Emmanuelle Faubert performed minigene study, Severine Nony made analytical technic, Céline Renoux made genetic diagnosis, Manuel D. Carcao gave clinical information about patients, Pascale Fanen designed minigen assay, Benoît Funalot performed genetic analysis, Lamisse Mansour-Hendili and Philippe Joly wrote and directed the study.

ACKNOWLEDGEMENTS

None.

FUNDING INFORMATION

None.

CONFLICT OF INTEREST STATEMENT

The authors have no competing interests.

DATA AVAILABILITY STATEMENT



Deidentified participant data are available upon reasonable request made to the corresponding author Dr Ariane Lunati-Rozie.


PATIENT CONSENT STATEMENT

All patients provided written informed consent.




PERMISSION TO REPRODUCE MATERIAL FROM OTHER SOURCES

Not applicable.

Ariane Lunati-Rozie^{1,2}
 Alexandre Janin^{3,4}
 Emmanuelle Faubert^{1,2}
 Severine Nony⁴
 Céline Renoux^{4,5} 
 Manuel D. Carcao⁶ 

Pascale Fanen^{1,2}
 Benoît Funalot^{1,2}
 Lamisse Mansour-Hendili^{1,7}
 Philippe Joly^{4,5,8} 

ORCID

Céline Renoux  <https://orcid.org/0000-0002-7263-805X>
 Manuel D. Carcao  <https://orcid.org/0000-0001-5350-1763>
 Philippe Joly  <https://orcid.org/0000-0002-2351-9441>

¹Département de Biochimie-Biologie Moléculaire,
 Pharmacologie, Génétique Médicale, AP-HP, Hôpitaux
 Universitaires Henri Mondor, Créteil, France

²Université Paris-Est Créteil, INSERM, IMRB, Créteil,
 France

³Institut NeuroMyoGène, Laboratoire Physiopathologie
 et Génétique du Neurone et du Muscle, CNRS UMR
 5261 -INSERM U1315 - Université de Lyon - Université
 Claude Bernard Lyon 1, Lyon, France

⁴Service de Biochimie et de Biologie Moléculaire,
 Centre de Biologie et de Pathologie Est, Hospices Civils
 de Lyon, Bron, France

⁵Laboratoire Interuniversitaire de Biologie de la
 Motricité (LIBM) EA7424, Equipe "Biologie vasculaire
 et du globule rouge", Université Claude Bernard Lyon
 1, COMUE, Lyon, France

⁶Paediatric Haematology and Oncology, Hospital for
 Sick Children, Toronto, Ontario, Canada

⁷IMRB Equipe Pirenne, Laboratoire d'excellence
 LABEX GRex, Université Paris-Est Créteil, Créteil,
 France

⁸Laboratoire d'Excellence du Globule Rouge, Labex
 GR-Ex, Université Paris, PRES Sorbonne, Paris, France

Correspondence

Ariane Lunati-Rozie, Département de Biochimie-
 Biologie Moléculaire, Pharmacologie, Génétique
 Médicale, AP-HP, Hôpitaux Universitaires Henri
 Mondor, Créteil, France.

Email: ariane.lunati-rozie@aphp.fr

Lamisse Mansour-Hendili and Philippe Joly share
 effectively the same position.

REFERENCES

1. Narla J, Mohandas N. Red cell membrane disorders. *Int J Lab Hematol*. 2017;39(S1):47–52.
2. Mansour-Hendili L, Aissat A, Badaoui B, Sakka M, Gameiro C, Ortonne V, et al. Exome sequencing for diagnosis of congenital hemolytic anemia. *Orphanet J Rare Dis*. 2020;15(1):180.
3. on behalf of the ACMG Laboratory Quality Assurance Committee, Richards S, Aziz N, Bale S, Bick D, Das S, et al. Standards and guidelines for the interpretation of sequence variants: a joint consensus recommendation of the American College of Medical Genetics and Genomics and the Association for Molecular Pathology. *Genet Med*. 2015;17(5):405–23.
4. Tole S, Dhir P, Pugi J, Drury LJ, Butchart S, Fantauzzi M, et al. Genotype–phenotype correlation in children with hereditary spherocytosis. *Br J Haematol*. 2020;191(3):486–96.
5. Wu C, Xiong T, Xu Z, Zhan C, Chen F, Ye Y, et al. Preliminary study on the clinical and genetic characteristics of hereditary spherocytosis in 15 Chinese children. *Front Genet*. 2021;12:652376.
6. Gallagher PG, Maksimova Y, Lezon-Geyda K, Newburger PE, Medeiros D, Hanson RD, et al. Aberrant splicing contributes to severe α -spectrin-linked congenital hemolytic anemia [Internet]. 2019 [cité 2019 juin 11]. Disponible depuis: <http://www.jci.org/articles/view/127195/pdf>

SUPPORTING INFORMATION

Additional supporting information can be found online in the Supporting Information section at the end of this article.